


FVIII Binding to PS Membranes Differs in the Activated and Non-Activated Form and Can Be Shielded by Annexin A5

Hanna Engelke,[†] Svenja Lippok,[†] Ingmar Dorn,[‡] Roland R. Netz,[§] and Joachim O. Rädler^{*,†}

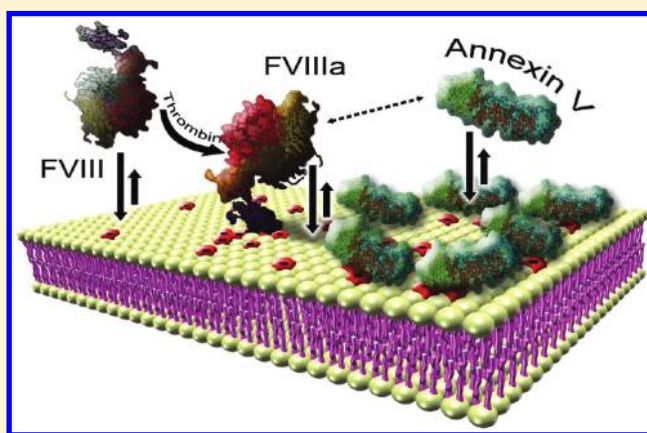
[†]Center for NanoScience (CeNS) and Fakultät für Physik, Ludwig-Maximilians-Universität, Geschwister-Scholl-Platz 1, D-80539 München, Germany

[‡]Bayer Technology Services GmbH, 51368 Leverkusen, Germany

[§]Technische Universität München, 85748 Garching, Germany

 Supporting Information

ABSTRACT: Binding of Factor VIII to phosphatidylserine (PS)-expressing platelets is a key process in the intravascular pathway of the blood coagulation cascade. Activated by thrombin, FVIIIa acts as a cofactor on the surface of platelets. It is under debate whether and how annexin A5 influences FVIIIa binding to platelets. Here, we investigate FVIII binding to PS-containing vesicles as model platelets and its interplay with annexin A5 in buffer using fluorescence correlation spectroscopy (FCS). We find that activated FVIIIa, in contrast to inactivated FVIII, exhibits a striking binding anomaly as a function of PS content, marked by a sharp maximum of the binding constant around 11% PS, which is close to the natural PS content of platelets. Furthermore, we show that the addition of annexin A5 can both increase or decrease this FVIIIa binding depending on whether the relative PS content is lower or higher than the maximum binding value. We demonstrate in theory that the observed binding diagram supports the hypothesis that annexin shields PS, indicating a possible indirect regulatory role of annexin A5 in blood coagulation. The overall PS- and annexin-dependent binding behavior of activated FVIIIa is preserved in experiments in blood plasma, confirming the validity of our results under more physiological conditions.



INTRODUCTION

Factor VIII is a key cofactor in the blood coagulation cascade. Its inherited deficiency in humans causes a severe dysfunction in hemostasis, leading to the bleeding disorder known as hemophilia A. A decisive event in the blood coagulation cascade is the binding of activated FVIIIa to phosphatidylserine (PS)-exposing platelets. FVIII is activated by thrombin, which releases FVIII from its carrier, the von Willebrand factor by cleaving off its B-domain. FVIIIa subsequently forms the tenase complex on the surface of the platelet membrane with the enzyme factor IX. Recently, it was found that activated FVIIIa exhibits enhanced binding affinity to platelets, as compared to its inactive form.¹ One important blood protein, that is believed to influence blood coagulation, is annexin A5, which binds to PS-containing membranes in a calcium dependent manner.^{2–5} Annexin A5 binds to endothelial cells, leading to immediate effects on thrombin formation.⁶ It was shown that antiphospholipid antibodies, which inhibit annexin A5 binding to phospholipids, accelerate plasma coagulation.⁷ Furthermore, the inhibitory effect of annexin A5 on the binding of FVIII to platelets seems to be specific to activated FVIIIa and not significant for inactivated FVIII.⁸

Additional evidence has been reported regarding the anti-coagulant effect of annexin A5, although the mechanism of this effect remains unclear.² It was proposed that the formation of a two-dimensional annexin A5 crystal lattice leads to a reduction of lateral movement of membrane-bound coagulation factors, and hence a reduction of the kinetic rates in the membrane-based coagulation pathway.⁹ Alternatively, annexin A5 is suggested to compete with coagulation factors for binding sites on the platelet membrane, thereby inhibiting their membrane-based interaction, as schematically depicted in Figure 1.

Therefore, a quantitative understanding of FVIII and annexin A5 binding to platelet membranes and their possible interference is important for quantitative modeling of the coagulation cascade. Generally, a systems biology approach to hemostasis has the potential to leverage medical and pharmaceutical research.¹⁰ However, the complexity of the biochemical network represents a formidable challenge. Prerequisites for quantitative modeling

Received: May 25, 2011

Revised: September 28, 2011

Published: September 28, 2011

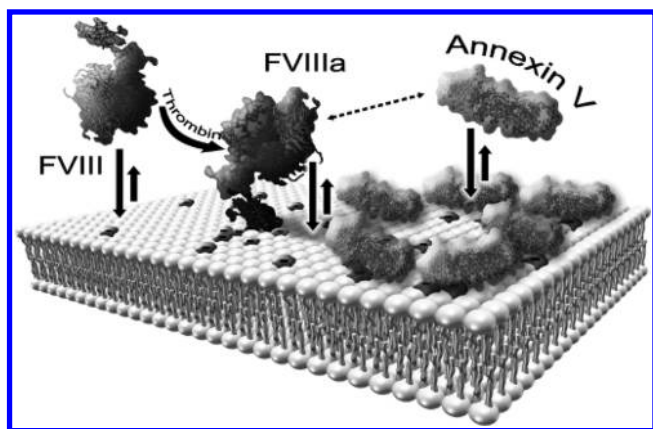


Figure 1. Schematic illustration of FVIII activation and binding to a phosphatidylserine (PS)-containing membrane. Annexin A5 is shown to compete for PS binding sites.

are the knowledge of the binding constants and reaction rates. Here, we focus on the lipid membrane related reactions of FVIII in the blood coagulation cascade. For such protein–membrane interactions, lipid membrane composition and local lipid phase segregation play a regulatory role. This kind of regulation by spatial organization has been shown, for instance, for binding to membranes containing the polyvalent acidic lipid phosphatidylinositol-4,5-bisphosphate (PIP₂) and on T-cell membranes, which form microdomains induced by protein binding.^{11,12,22} However, these parameters are not fully captured in the current simulations and models. Binding of inactivated FVIII to PS-model membranes occurs in a charge dependent manner through a region in the C2 domain, which is enriched by four basic and three hydrophobic residues.^{13,14} For activated FVIIIa, however, binding and, particularly, its dependence on negative charge, i.e., the PS content, has not yet been investigated. Likewise, there is no support by quantitative data for the hypothesis of competitive binding of FVIII and annexin to negatively charged membranes.

In this Article, we measure the binding of FVIII and FVIIIa to PS-containing membranes as well as investigate the mechanism of how annexin influences FVIIIa binding to membranes, as schematically shown in Figure 1. We use fluorescence correlation spectroscopy (FCS) to study FVIII and FVIIIa interacting with PS-containing vesicles as model membranes. FCS measures diffusion times and can discriminate freely diffusing from vesicle-bound proteins based on the size dependence of diffusion, as further explained in the Supporting Information.^{15,16} We measure binding isotherms of FVIII binding to vesicles in consecutive titration experiments and study the binding characteristics of FVIII and FVIIIa as a function of the PS content of the membrane. For inactivated FVIII, we find a continuous increase of the binding constant with increasing PS content. In contrast, for activated FVIIIa, an anomaly in binding and an extremely enhanced sensitivity to the PS content was observed at the physiological PS content of activated platelets. The underlying molecular mechanism can be explained by binding of charged lipids to discrete protein binding sites and repulsion from neutral protein sites. As we will show in this Article, the binding anomaly of FVIIIa allows for an efficient regulatory role of annexin A5, if annexin A5 competes for binding to PS and hence changes the effective PS concentration sensed by FVIIIa.

EXPERIMENTAL PROCEDURES

Sample Preparation. Recombinant FVIII (Kogenate-FS) was obtained from Bayer HealthCare and labeled using Alexa 488-tagged ESH2 antibodies (American Diagnostica). (For additional information, see the Supporting Information.) This labeling method avoids aggregates that we found to be introduced by direct labeling of FVIII, and it allows for flexible labeling without direct chemical modification of the protein. Prior to labeling, FVIII was activated through a 30 min incubation with human thrombin at 37 °C, as described in Ahmad et al.⁸ Antibody binding tests (see the Supporting Information) showed that activation was successful. FVIII and antibodies were diluted at concentrations of 110 and 10 nM, respectively, in citrate buffer (50 mM, pH 6.7, with 1 mM CaCl₂, 40 μg/mL Tween 80). 100 nm unilamellar vesicles were prepared by the extrusion of 1-palmitoyl-2-oleoyl phosphatidylcholine (POPC) and 1-palmitoyl-2-oleoyl-*sn*-glycero-3-phosphatidylserine (POPS) (Avanti Polar Lipids) in citrate buffer.

For experiments with annexin A5, annexin (Sigma Aldrich) was mixed with vesicles in citrate buffer with CaCl₂ added at a concentration of 12.5 mM. Control experiments were performed, which proved that FVIII binding does not change upon addition of this amount of CaCl₂. Annexin A5 (Sigma Aldrich) was incubated with vesicles and CaCl₂ for 2 min prior to the addition of FVIII. Cross-correlation experiments were performed with Alexa 647-labeled annexin A5 (Invitrogen) on supported lipid bilayers, which were prepared using the sonication technique.²¹ FVIII-deficient plasma in citrate buffer (American Diagnostica) was added to the buffer solution, yielding a 1:1 buffer:plasma mixture. FXa inhibitor (Tenstop, American Diagnostica) was added to prevent possible tenase complex formation on the vesicles.

Instrumentation. FCS measurements were performed on an Axiovert 200 microscope equipped with a ConfoCor 2 unit (Carl Zeiss, Jena, Germany). For excitation, an argon ion laser at 488 nm with an average power of 15 μW on the sample was used. Fluorescence emission was filtered from the excitation light using a 525/25 bandpass filter. The objective used was a 40× (NA = 1.2) water immersion apochromat (Carl Zeiss Jena, Germany). Samples were measured in eight well LabTek I chamber slides (Nunc, Rochester, NY). For cross-correlation experiments with Alexa 647-labeled annexin A5, a HeNe laser (633 nm) and a long-pass 650 filter were added to the setup. Correlation and analysis were performed using the ConfoCor 2 software. FCS data analysis is in accordance with Rusu et al.,¹⁶ and is described in greater detail in the Supporting Information.

RESULTS

FVIII and FVIIIa Binding to PS Vesicles. We measured binding of FVIII and FVIIIa to vesicles containing different PS concentrations, as shown in Figure 2a. In FCS, fluorescence intensity fluctuations are recorded from the diffusion of fluorescently labeled proteins through an open focal illumination volume. The autocorrelation function of the fluorescence time series exhibits a characteristic decay representing the average time the molecules need to diffuse across the focal volume (Figure 2b). For proteins binding to the 100 nm vesicles, which are larger than the freely diffusing proteins, the diffusion time increases. This leads to the evolution of the autocorrelation functions depicted in Figure 2b. Each of the intermediate autocorrelation functions

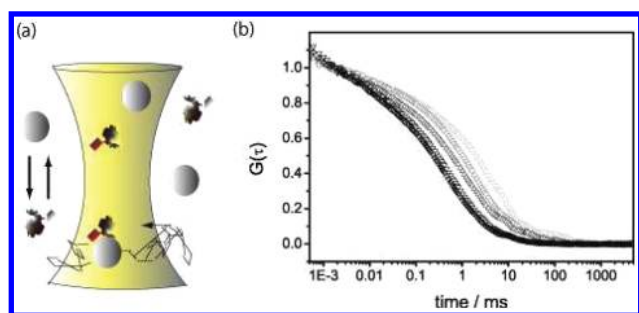


Figure 2. (a) Fluorescence correlation spectroscopy (FCS) detects FVIII binding to vesicles through the measurement of the diffusion time of fluorescently labeled FVIII across an open illumination volume. (b) Evolution of the time autocorrelation functions of FVIIIa as vesicles with 10% PS mol fraction are added. The fraction of vesicle-bound, slowly diffusing FVIIIa to the freely diffusing FVIIIa increases with lipid concentration from dark to light gray.

can be fitted by a sum of two autocorrelation functions corresponding to the fraction of bound and unbound proteins.¹⁶ Consequently, the fraction of bound proteins can be obtained from the measured correlation function using appropriate fits (for details, refer to the Supporting Information). For FCS measurements, the protein needs to be fluorescently labeled. Here, FVIII was indirectly tagged using the fluorescently labeled antibody ESH2, which binds to FVIII without obstructing the capability of FVIII to bind PS-containing membranes.¹⁷ As a control, we also used FVIII tagged with the antibody ESH8. We measured the fraction of bound FVIII and FVIIIa as a function of lipid concentration. Figure 3a shows an example of an isotherm that was obtained from a measurement on FVIII binding to vesicles of 10% PS content. These isotherms were recorded for lipid compositions with varying amounts of PS. In each case, we find binding isotherms described by

$$f_{\text{bound}}(L) = \frac{K(\text{PS}) \cdot L}{1 + K(\text{PS}) \cdot L} \quad (1)$$

where $K(\text{PS})$ denotes the molar partition coefficient and L the molar lipid concentration in solution. $K(\text{PS})$ describes the distribution of free and bound FVIII, and hence its binding constant to the lipid membrane as a function of its relative PS content. Note that the binding isotherm is sometimes fitted with reference to a bimolecular binding model, assuming a discrete number of lipids per binding site.¹³ In the binding site description, the concentration of binding sites $L^* = L/n$ is related to the lipid concentration through the number of lipids per binding site, n . Consequently, the dissociation constant, K_D , according to the discrete binding model and $K(\text{PS})$ are related by $n \cdot K_D = K^{-1}(\text{PS})$. The PS content dependence of FVIII binding to membranes is plotted on a semilog scale in Figure 3b. The molar partition coefficient increases with increasing strength of binding, showing that binding increases continuously with increasing PS content for inactivated FVIII. For vesicles without PS, no significant binding could be detected within the range of concentrations studied. The measured $K_{\text{FVIII}}(\text{PS})$ values are in exact agreement with the previously reported data by Gilbert et al. using resonance energy transfer.¹³ The line represents a fit indicating an exponential increase within the range of PS contents studied.

Interestingly, binding of activated FVIIIa notably deviates from this behavior. Figure 3b shows the strongly peaked dependence of FVIIIa binding on the membrane PS content. Binding sharply

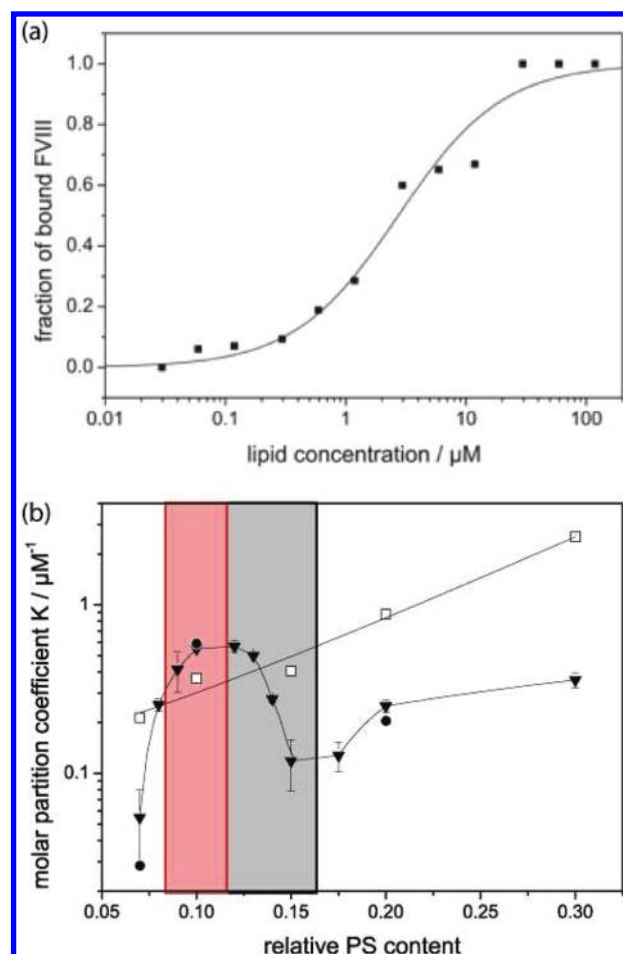


Figure 3. (a) Binding isotherm of FVIII binding to vesicles of 10% PS content. (b) The molar partition coefficient (binding constant), $K(\text{PS})$, of activated (filled triangles) and nonactivated (open squares) FVIII. The black round data points indicate control experiments with activated FVIIIa labeled with ESH8 instead of ESH2. The range of physiological mol percentage of PS in activated platelets is marked in red. The region of the anomalous decrease in the binding constant with increasing PS content is indicated by the gray region. Comparison of the FVIII and FVIIIa data shows the strong deviation of FVIIIa from common binding behavior.

increases up to $K_{\text{FVIIIa}}(\text{PS}) = 0.6 \mu\text{M}^{-1}$ at a relative PS concentration of 11%, which exceeds the binding of inactivated FVIII by 100%. Surprisingly, the binding constant of activated FVIII decreases beyond this point, and reaches a minimum at about 17% PS content ($K_{\text{FVIII}}(\text{PS}) = 0.1 \mu\text{M}^{-1}$). This behavior must be considered anomalous, since the general understanding implies that binding increases with PS content due to electrostatic interaction. In order to confirm this result, we have measured the binding constant using optical thermophoresis as an independent second technique and obtained agreement within the experimental accuracy (see the Supporting Information). It is remarkable that the observed anomaly falls within the physiological range of PS content on the outer membrane of activated platelets. A comparison of the molar partition coefficients of inactivated and activated FVIII reveals that activated FVIII shows weaker binding than inactivated FVIII over most of the PS content range, except for this narrow region of the peak between 8 and 14%.

Theoretical Modeling of FVIIIa Binding. The binding behavior of FVIII differs remarkably depending upon whether it is activated or not. In particular, the affinity of FVIIIa exhibits a maximum as a function of PS content, which is unusual, as it implies that beyond an optimal PS content the protein membrane interaction, that has a significant attractive electrostatic contribution, decreases despite the increasing surface charge of the lipid membrane. In electrostatic theory, the interactions of oppositely charged bodies, i.e., protein and membrane, increase monotonously with increasing charge of either component. This is indeed the case for the interaction of inactivated FVIII with PS membranes.^{1,19} The existence of a maximum for FVIIIa is hence a principal challenge to the mechanism of FVIII binding to PS membranes. In the following, we present a simple statistical model that describes this phenomenon. It is well-known that the electrostatic interaction of the PS moiety in the lipid membrane plays a key role in FVIII binding. First, crystallography data show three residual positive charges on the membrane facing side of the protein. Second, when the protein binds to the membrane, its surface covers a distinct area of the membrane, which can be estimated to correspond to about 25 lipids. A fraction Φ of the lipids are charged PS lipids, and it is assumed that the binding energy is composed out of the binding energy of these charged constituents. The situation is depicted schematically in Figure S1 of the Supporting Information. We now introduce the very assumption that discriminates the activated and inactivated form in our model. In the nonactivated form, we assume that the electrostatic charge of the protein is equally distributed over the contact area and hence all $M = 25$ lipid sites have the same chemical free energy for a PS lipid. The reason for this could be that charges are buried by the B-domain of the protein or that there is a water layer between the protein and lipid bilayer. In contrast, in the case of activated FVIII, we assume the existence of three discrete binding sites for PS, as depicted in Figure S1 of the Supporting Information. In both cases, the binding constant, K , of the protein is determined from the statistical mean of the free energy, F , considering all possible configurations of charged lipids underneath the protein.

$$K = N \exp(-F/kT) = N \cdot Z(\tilde{\mu}) = N \cdot \sum_{m=1}^M P_M(m) e^{m\tilde{\mu}} \quad (2)$$

where N is a constant normalization factor and $Z(\tilde{\mu})$ denotes the partition function, with $P_M(m)$ being the probability that m lipids in the contact area are charged and $\exp(m\tilde{\mu})$ its statistical weight (for the explicit presentation of $P_M(m)$, see the Supporting Information).

For the electrostatic binding of inactivated FVIII to membranes, we assume that each charged lipid under the protein contributes an equal amount of $\tilde{\mu}kT$ to the binding energy. Hence, binding increases with an increasing amount of charged lipids underneath the protein. The fit in Figure S2 of the Supporting Information with only the energy contribution per lipid $\tilde{\mu}$ and the normalization factor N as free fit parameters shows that this model reveals the PS dependence of the inactivated FVIII well.

The discrete binding of activated FVIII is modeled by discrimination of the energy contributions of charged lipids at charge binding sites and those at neutral sites of the protein.

Negatively charged lipids at charge binding sites are attracted and hence contribute a positive amount of $\tilde{\mu}_1 kT$ to the binding

energy. Charged lipids, which are not at these sites, are repulsed and their contribution $\tilde{\mu}_2 kT$ to the binding energy is negative. The reason for this could be the entropic confinement of the counterions. The contribution of the charged lipids at charge binding sites leads to an increase of binding with increasing fraction of charged lipids at low PS concentrations up to a certain value, beyond which the repulsion at neutral sites dominates, resulting in a decrease of binding with increasing PS content of the membrane. The discrimination of these two different energy contributions leads to one additional parameter, $\tilde{\mu}_2$, and the probability function $P_M(m)$ splits into the probabilities $P_K(k)$ to find k charged lipids at the K charge binding sites and $P_L(l)$ to find l charged lipids at the $L = M - K$ neutral sites (for details, see the Supporting Information). Figure S2 of the Supporting Information shows that this discrete binding model reproduces the peak in the PS dependence of activated FVIII with only one additional parameter as compared to the model for inactivated FVIII. However, it reveals only the peak and it fails to describe the increase of the binding constant at high PS contents. This increase signals cooperative effects, which we implement in the model by addition of a quadratic term $l^2 \varepsilon$ in the binding energy per charged lipid at noncharge binding sites. The dashed line in Figure S2 of the Supporting Information, which was obtained by the model including this extension, reveals the increase of binding at high PS contents. The experimental data for FVIIIa are more sharply peaked around the maximum than the theoretical model. The agreement could be improved by including higher order terms also for the PS lipids underneath charge sites, which we did not pursue in this paper.

Annexin A5 Can Both Reduce and Increase Binding of FVIIIa to PS Membranes. As annexin-A5 is supposed to affect the binding of FVIII to platelets, we study its influence on the binding of FVIII to membranes quantitatively by incubating the vesicles with annexin-A5 prior to the binding experiments with FVIII. In the case of inactivated FVIII, annexin-A5 had a weak but by trend decreasing influence on the binding. In contrast, FVIIIa binding was strongly influenced by the presence of annexin A5 even at low annexin concentrations of $4 \mu\text{M}$. In fact, the full binding diagram as a function of both PS content and annexin concentration revealed a multifaceted behavior, as shown in Figure 4a. We note that the addition of annexin can both reduce and increase the binding of FVIIIa, depending on the PS content of the membrane. The binding of FVIIIa to vesicles containing 10% PS is continuously reduced with increasing annexin concentration up to full inhibition (Figure 4b). When vesicles of a relative PS content of 15% were used, however, the inhibition characteristic disappears. In this case, preincubation of the vesicles with annexin enhances binding up to a maximum value. At concentrations higher than this maximum, a reduction of FVIIIa binding to the vesicles is again observed (Figure 4c). Separate experiments on annexin binding to vesicles showed that this does not lead to vesicle aggregation and hence does not lead to these results by interfering with the FCS measurements.

Quantitative Model of Annexin Interaction. This change in the FVIIIa binding behavior in the presence of annexin A5 can be explained by an extended competitive inhibition model. It is generally assumed that annexin competes with FVIII for binding to PS lipid. We first demonstrate that, however, ordinary competitive binding does not fully describe the data. Competitive inhibition describes the interaction of a ligand and a receptor in the presence of a second ligand competing for binding to the same receptor. The competition for binding sites is based on

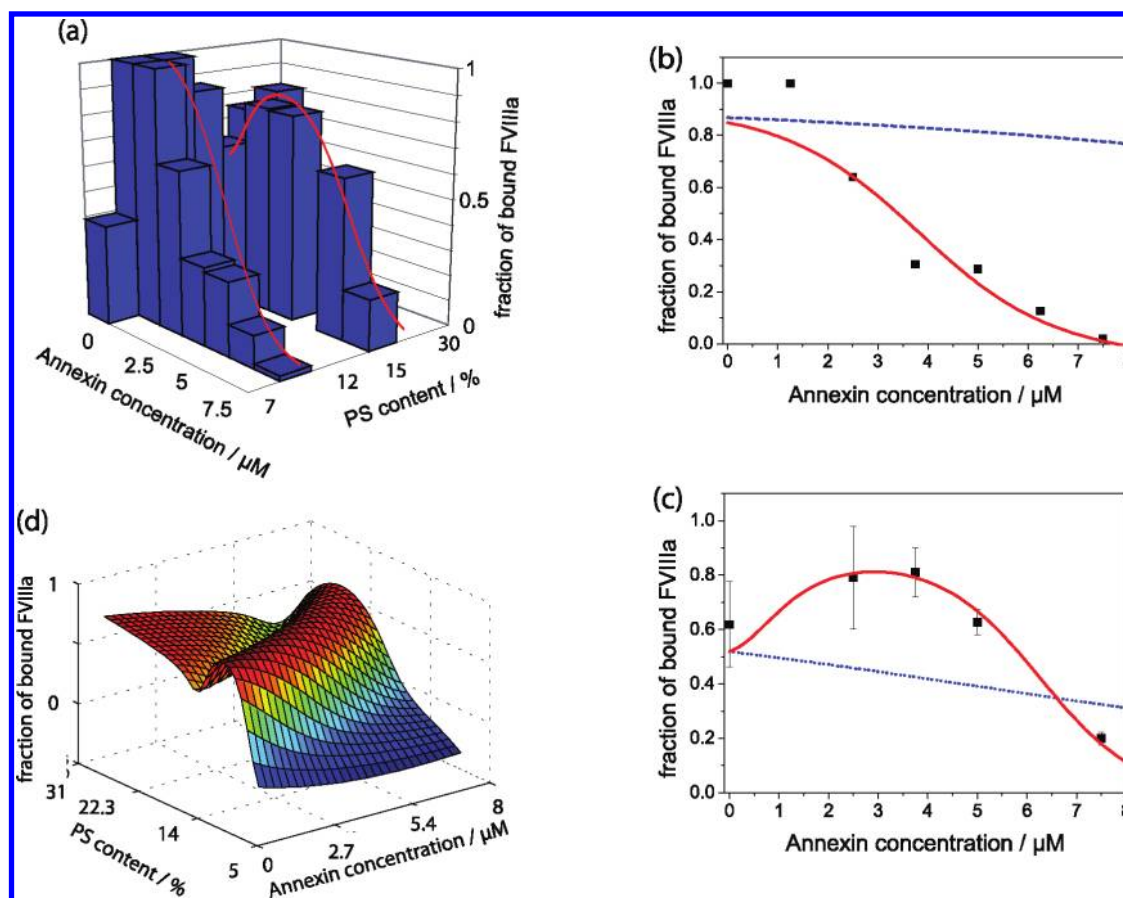


Figure 4. (a) 3D plot of the measured fraction of membrane-bound FVIIIa as a function of PS mol fraction and annexin A5 concentration. Cross-sectional plot of part a showing the influence of annexin A5 on FVIIIa binding to PS membranes at a PS content of 10% (b) and 15% (c). The blue dashed lines indicate a fit according to the simple competitive model, while the red full lines represent a fit following the extended shielding model. (d) Three-dimensional binding plot showing shielding model simulations of the PS content and annexin A5 concentration dependence of FVIIIa binding to membranes at a constant lipid concentration.

mass action, and hence, in our case, the binding of annexin A5 to PS reduces the absolute number of available PS binding sites for FVIIIa. This leads to an effectively reduced lipid concentration, $L_{\text{eff}}(A) = L - L_A$, with L_A being the number of lipids shielded by annexin A5. Replacing L by $L_{\text{eff}}(A)$ in eq 1, we obtain the fraction bound of FVIII for competitive inhibition. This model, however, fails to describe the strong inhibition we measured for membranes with 10% PS content quantitatively, as seen in Figure 4b, where the blue dashed line represents a fit according to the competitive inhibition model. Moreover, the standard inhibition model can only explain the decrease in binding but not the enhanced binding measured for membranes with 15% PS content (Figure 4c).

We introduce now an extended competitive inhibition model, which assumes that annexin-A5 also modifies the binding constant $K_{\text{FVIIIa}}(\text{PS})$ due to the fact that PS lipid is shielded. The modified binding constant $K_{\text{FVIIIa}}(\text{PS}_{\text{eff}}(A))$ is described by an effective PS content, $\text{PS}_{\text{eff}}(A) = \text{PS}_0 \cdot (1 - \alpha A_b)$, where the amount of annexin bound (A_b) is given by the binding constant, K_A , of annexin A5 to the membrane (see the Supporting Information). In addition, the molar shielding efficiency, α , was introduced to quantify the efficiency of relative PS content reduction per mol annexin. A shielding efficiency of $\alpha = 0.1 \mu\text{M}^{-1}$, for instance, implies that 1 μM annexin reduces the relative PS content by 10%. Due to the sensitivity of FVIIIa binding to the PS content of

membranes described above, a reduction of the relative PS content induces dramatic changes to the binding constant $K_{\text{FVIIIa}}(\text{PS})$, causing either the enhanced or reduced binding of FVIIIa. A quantitative description of the fraction of bound FVIIIa as a function of annexin A5 is given by

$$f_{\text{bound}}(\text{PS}, A) = \frac{K(\text{PS}_{\text{eff}}(A)) \cdot L_{\text{eff}}(A)}{1 + K(\text{PS}_{\text{eff}}(A)) \cdot L_{\text{eff}}(A)} \quad (3)$$

Note that eq 3 contains only one unknown parameter, since we can use both the measured dependence, $K_{\text{FVIIIa}}(\text{PS})$, and the measured binding constant of annexin, K_A , which determine the effective quantities (for more details, refer to the Supporting Information). Equation 3 consistently describes the measured concentration dependence of the bound fraction (solid lines, Figure 4b and c). The strength of the model is the fact that only one adjustable parameter, the shielding efficiency α , is required, and has to be consistent with all measurements. The fact that both 10% PS and 15% PS data sets are well-described using the same α confirms the validity of the model. To further elaborate on the full phase diagram of the binding behavior, we plotted the theoretical landscape of binding as a function of PS and annexin A5 concentration (Figure 4d). The anomaly of the PS dependence of FVIIIa binding to membranes allows for inhibition and enhancement of binding, which occurs upon the reduction of the effective PS

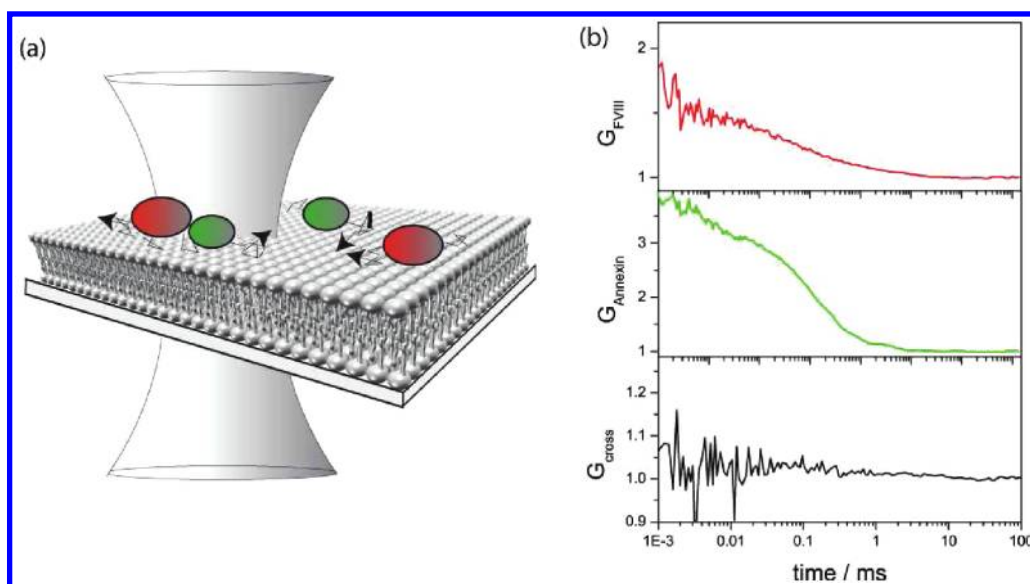


Figure 5. (a) Schematic diagram of the two-dimensional two-color cross-correlation FCS measurement on a supported membrane. (b) Autocorrelation curves of activated FVIII (red line) and annexin A5 (green line) on a supported lipid bilayer. No cross-correlation (black line) between annexin A5 and activated FVIII can be detected, indicating that these do not directly interact. The diffusion coefficient of activated FVIII is not influenced by annexin A5, and is measured to be approximately $10 \mu\text{m}^2 \text{s}^{-1}$ for both.

content through the addition of annexin. The shielding model is thus able to qualitatively and quantitatively explain the mechanism of interaction of annexin and FVIIIa binding to membranes.

Cross-Correlation Experiments. A key component of the inhibition model is the assumption that there is no direct interaction between annexin and FVIIIa. All annexin interference occurs indirectly via PS shielding, which then modulates the binding affinity of the membrane to FVIII. In order to test this hypothesis, we performed dual color cross-correlation experiments on supported membranes, as schematically depicted in Figure 5a. In this experiment, FVIIIa is labeled with green fluorescent-tagged antibody, while annexin is labeled with a red fluorescent-tagged antibody. Fluorescence cross-correlation, through the two-color coincidence, can differentiate between the diffusion of free proteins and correlated protein clusters through the focal spot. Distinct autocorrelation curves are obtained for both annexin and FVIIIa, yielding a diffusion coefficient of about $10 \mu\text{m}^2 \text{s}^{-1}$. This is approximately equal to the diffusion coefficient of lipids in the membrane (Figure 5b). Nevertheless, the cross-correlation shows a flat time dependence, indicating that the diffusion of annexin and of FVIIIa are not correlated. Comparison of the diffusion coefficients of each protein on a membrane in the presence and absence of the other indicates that the diffusion of one is not influenced by the other. Furthermore, the homogeneity of the intensity signal obtained in these experiments shows the absence of aggregates and their possible influence on the binding. Addition of calcium and chelation of calcium with EDTA lead to a change of the ratio of bound FVIIIa and bound annexin A5, whereas addition of neither EDTA nor calcium changed the amount of bound FVIIIa in the absence of annexin A5. This was used to fine-tune the concentrations of bound FVIIIa and annexin A5 in the cross-correlation experiments and is a further proof of the modulation of FVIIIa binding by annexin A5.

Experiments in Plasma. To see if our experimental results are valid under *in vivo* conditions, we repeated the experiments in

FVIII-deficient blood plasma. Since plasma is a strongly scattering, crowded medium, FCS measurements face an experimental hurdle that needs to be addressed in the analysis. We have recently described a procedure on the required corrections for both the scattering and crowding effects in FCS data analysis.¹⁸ Taking these effects into account, we were able to measure FVIII binding to vesicles containing 15% PS (see the Supporting Information). The first satisfying finding is that the molar partition coefficients of FVIIIa binding to LUVs (in the absence of annexin A5) in plasma are consistent with those obtained in buffer. Second, preincubation of the membranes with annexin A5 in plasma leads to the same characteristic enhancement and inhibition behavior observed in buffer. However, the absolute concentration of annexin A5 necessary to reach the same level of inhibition differs in plasma and buffer by a factor of 4, as shown by the rescaling of the theoretical prediction for the data in buffer (solid line, Figure 6) by a factor of 4 (dashed line, Figure 6).

DISCUSSION

We studied the binding of inactivated and activated FVIII to PS-containing phospholipid model membranes. The molar partition coefficient of inactivated FVIII is found to exhibit an exponential increase as a function of mol percentage PS, which is consistent with data from Gilbert et al.¹³ and Bardelle et al.¹⁹ This increase is caused by electrostatic interaction, which is proportional to the mol percentage PS in cases where there is low surface charge density.²⁰ The molar partition coefficients for FVIIIa, in contrast, were found to exhibit a pronounced binding anomaly consisting of a peaked binding affinity in the region of about 12% PS. This anomaly is reported for the first time, and a possible molecular mechanism is presented employing binding of charged lipids to a discrete number of protein binding sites.

Factor VIII is activated by thrombin through the site-specific cleavage of both the heavy and light chains, resulting in the separation of the A1 and A2 domains, as well as the release of the B-domain. *In vivo*, these conformational changes lead to the

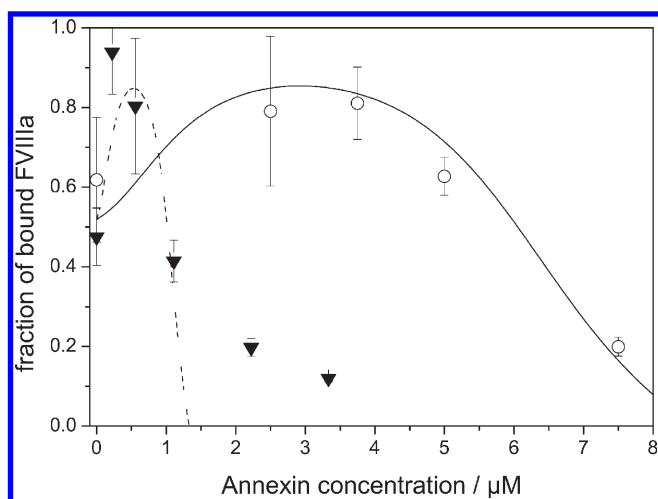


Figure 6. Comparison of the regulation of FVIIIa binding by annexin A5 in buffer (open circles) and in plasma (full triangles). The experiments in buffer are fitted according to the shielding model (full line), while the data in plasma can be described by the same theoretical dependence, when it is rescaled by a factor of 4 (dashed line).

dissociation of FVIII from the von Willebrand factor.¹ It is also believed that FVIII undergoes a conformational change in the C2 membrane-binding domain. We assumed that the release of the B-domain and possibly the associated conformational changes lead to exposition of the charge binding sites to the membrane and consequently to the observed enhancement of FVIIIa binding to membranes with an approximate composition of 12% molar content PS. It is noteworthy to mention that this binding characteristic of FVIIIa is also observable in blood plasma. The fact that binding of activated FVIII exceeds the binding of FVIII only in a narrow region of PS content, which coincides with the physiological PS content, might be important, since it allows for the selective binding of FVIIIa when injury occurs.

The experimental data of FVIIIa binding in the presence of annexin A5 seem to support an extended inhibition model proposed here, which assumes that annexin effectively reduces the PS content by shielding PS lipids upon binding. The partition coefficient of FVIIIa is shifted according to the reduced PS content, which, due to the unusual nature of the binding isotherm, results in an increase or decrease in binding affinity, depending on the actual PS concentration. The question arises if the characteristic of FVIIIa binding to vesicles also holds true for binding to platelets in circulation. Ahmad et al.⁸ measured FVIII and FVIIIa binding to platelets corresponding to molar partition coefficients of 0.56 and $0.8 \mu\text{M}^{-1}$, respectively, close to the values reported here for liposomes having a PS content approximately comparable to the physiological levels (10%). Our finding that FVIIIa exhibits stronger binding compared to FVIII in the physiological range is also consistent with results obtained for platelet binding.^{1,8} Furthermore, FVIIIa binding to platelets is inhibited by annexin A5, which is in accordance with the findings from our model system. These results collectively confirm that PS-containing vesicles serve as a suitable model system for platelets, and that charge shielding, which reduces the effective charge of the membrane for FVIIIa, could be a mechanism for the involvement of annexin A5 in blood coagulation. Such a shielding mechanism explains the anticoagulant effect of annexin under

nonpathological physiological conditions, and predicts a possible procoagulant effect for platelets exhibiting PS levels exceeding 12%.

We demonstrate that our competition model describes an indirect influence of annexin A5 on the binding of FVIIIa via the effective concentration of PS. It is likely that this scheme can be extended to the interplay of many cofactors. Here, we presented first indications that the effect of annexin A5 on FVIIIa binding to model membranes is enhanced in the presence of blood plasma. This enhancement might be due to other cofactors such as Factor IX. Ahmad et al.,⁸ for example, reported an enhanced effect of annexin on FVIIIa binding to platelets in the presence of EGR-FIXa and FX. FCS allows for binding measurements in both buffer and plasma, and hence serves as a powerful tool for combinatorial binding studies. Such studies may ultimately allow the multidimensional cofactor landscape mapping of the membrane binding potential. This interplay of cofactor binding in membrane-based biochemical networks would be an important prerequisite to systems modeling of the blood coagulation cascade.

In conclusion, we have shown that the interaction of FVIIIa with PS membranes exhibits a highly unusual binding characteristic, which can be modulated by the presence of annexin. The binding of FVIII and FVIIIa is qualitatively described by a statistical binding model and in addition its modulation by annexin by an extended competition inhibition model. Our study thus exemplifies the importance of PS content as a regulatory signal within the blood coagulation cascade and the possible role of annexin as a passive regulator of the effective PS level in platelets. Measurements of FVIIIa binding in blood plasma are feasible using FCS and would allow the competitive or cooperative binding of other cofactors to be studied. A complete and quantitative description of the entirety of membrane-mediated cofactor interdependencies will be the subject of further research.

■ ASSOCIATED CONTENT

S Supporting Information. FCS analysis, antibody labeling, control experiments using optical thermophoresis, model of FVIII binding, and quantitative modeling of annexin regulation. This material is available free of charge via the Internet at <http://pubs.acs.org>.

■ AUTHOR INFORMATION

Corresponding Author

*E-mail: joachim.raedler@lmu.de.

■ ACKNOWLEDGMENT

Support from Bayer HealthCare, Berkeley, is gratefully acknowledged. H.E. also gratefully acknowledges the Elite Netzwerk Bayern for funding. J.O.R. and R.R.N. acknowledge support by the DFG through the excellence cluster NIM.

■ REFERENCES

- (1) Saenko, E.; Scandella, D.; Yakhyanev, A.; Greco, J. J. *Biol. Chem.* **1998**, *273*, 27918–27926.
- (2) Van Genderen, H.; Kenis, H.; Hofstra, L.; Narula, J.; Reutelingsperger, C. *Biochim. Biophys. Acta* **2008**, *1783*, 953–963.
- (3) Posokhov, Y.; Rodmin, M.; Lu, L.; Ladokhin, A. *Biochemistry* **2008**, *47*, 5078–5087.

- (4) Gerke, V.; Creutz, C.; Moss, S. *Nat. Rev. Mol. Cell Biol.* **2005**, *6*, 449–461.
- (5) Tait, J.; Gibson, D.; Smith, C. *Anal. Biochem.* **2004**, *329*, 112–119.
- (6) Van Heerde, W.; Poort, S.; van t’Veer, C.; Reutelingsperger, C.; de Groot, P. *Biochem. J.* **1994**, *302*, 305–312.
- (7) Rand, J.; Wu, X.; Andree, H.; Ross, J.; Rusinova, E.; Gascon-Lema, M.; Calandri, C.; Harpel, P. *Blood* **1998**, *92*, 1652–1660.
- (8) Ahmad, S.; Scandura, J.; Walsh, P. *J. Biol. Chem.* **2000**, *275*, 13071–13081.
- (9) Andree, H.; Stuart, M.; Hermens, W.; Reutelingsperger, C.; Hemker, H.; Frederik, P.; Willems, G. *J. Biol. Chem.* **1992**, *267*, 17907–17912.
- (10) Hockin, M.; Jones, K.; Everse, S.; Mann, K. *J. Biol. Chem.* **2002**, *277*, 18322–18333.
- (11) McLaughlin, S.; Murray, D. *Nature* **2005**, *438*, 605–611.
- (12) Golebiewska, U.; Gambhir, A.; Hangyas-Mihalyne, G.; Zaitseva, I.; Rädler, J. O.; McLaughlin, S. *Biophys. J.* **2006**, *91*, 588–599.
- (13) Gilbert, G.; Furie, B.; Furie, B. *J. Biol. Chem.* **1990**, *265*, 815–822.
- (14) Stoilova-McPhie, S.; Villoutreix, B.; Mertens, K.; Kernball-Cook, G.; Holzenburg, A. *Blood* **2002**, *99*, 1215–1223.
- (15) Rhoades, E.; Ramlall, T.; Webb, W.; Eliezer, D. *Biophys. J.* **2006**, *90*, 4692–4700.
- (16) Rusu, L.; Gambhir, A.; McLaughlin, S.; Rädler, J. *Biophys. J.* **2004**, *87*, 1044–1053.
- (17) Griffin, B. D.; Micklem, L. R.; McCann, M. C.; James, K.; Pepper, D. S. *Thromb. Haemostasis* **1986**, *55*, 40–46.
- (18) Engelke, H.; Dorn, I.; Rädler, J. *Soft Matter* **2009**, *5*, 4283–4289.
- (19) Bardelle, C.; Furie, B.; Furie, B.; Gilbert, G. *J. Biol. Chem.* **1993**, *268*, 8815–8824.
- (20) Ben-Tal, N.; Honig, B.; Peitzsch, R.; Denisov, G.; McLaughlin, S. *Biophys. J.* **1996**, *71*, 561–575.
- (21) Sackmann, E. *Science* **1996**, *271*, 43–48.
- (22) Douglass, A.; Vale, R. *Cell* **2005**, *121*, 937–950.